

Absorption of Positive Pions by Deuterium at 76 and 94 Mev*

HENRY L. STADLER

Institute for Nuclear Studies, The University of Chicago, Chicago, Illinois

(Received June 28, 1954)

The absorption of positive pions by liquid deuterium has been studied with scintillation counters, using a collimated pion beam from the Chicago synchrocyclotron. The differential cross sections for the production of protons at angles of 35°, 45°, 60°, and 90° are 1.189 ± 0.076 , 0.926 ± 0.058 , 0.643 ± 0.061 , and 0.442 ± 0.052 millibarns per steradian at 94 Mev and 1.010 ± 0.102 , 0.718 ± 0.081 , 0.431 ± 0.073 , and 0.300 ± 0.058 millibarns per steradian at 76 Mev in the center-of-mass system. The angular distribution can be represented by $a + \cos^2\theta$ with the following values of a : 0.268 ± 0.089 at 76 Mev and 0.388 ± 0.082 at 94 Mev. The total cross sections are 7.38 ± 1.21 millibarns at 76 Mev and 9.70 ± 1.03 millibarns at 94 Mev.

I. INTRODUCTION

THE theory of the pion absorption reaction, $\pi^+ + d \rightarrow p + p$, has been investigated by many authors¹⁻¹² and measurements of its cross section have been made at 23, 25, 40, and 53 Mev.^{13,14} (All energies mentioned in this section refer to pion energy in the center-of-mass system.) In addition, the inverse reaction, pion production, $p + p \rightarrow \pi^+ + d$, has been measured at a number of energies between 10 and 64 Mev.¹⁵⁻¹⁹ A review of the measurements of both the absorption and production reactions is contained in Rosenfeld.¹² The angular distributions at pion energies between 19 and 64 Mev appear to be representable as $d\sigma/d\omega \propto a + \cos^2\theta$, where a represents the isotropic contribution to the differential cross section. a seems to decrease from about 0.3 at 20 Mev to less than 0.2 at 64 Mev. This paper reports measurements of the angular distribution and total cross section of the absorption reaction at somewhat higher energies than have been studied before.

The following section describes the arrangement of the experimental equipment and explains how the reaction $\pi^+ + d \rightarrow p + p$ was measured without interference from any other processes. Section III indicates

the method of determining the energy and composition of the incident beam. Sections IV and V describe the liquid deuterium container and the counting equipment and Secs. VI and VII outline the calculation of the cross sections and angular distributions from the observed data.

II. EXPERIMENTAL METHOD

The measurement was made by bombarding liquid deuterium with positive pions from the Chicago synchrocyclotron. The arrangement is essentially the same as that used in previous work on pion scattering.²⁰ Pions are produced inside the cyclotron by the collision of 450-Mev protons with a beryllium target. The positive pions which are emitted backward from the proton beam direction are deflected outward by the cyclotron magnetic field and emerge from the vacuum chamber through a thin aluminum window. The fringe magnetic field of the cyclotron focusses some of the pions of each energy into a roughly parallel beam. Several of these beams of various nominal energies, 66 to 165 Mev, are allowed to pass through narrow channels cut through the 12-foot thick steel and concrete shield wall into the experimental room. For this experiment the 122-Mev pion channel was left open; all others were plugged with lead and steel blocks. The pion beam emerging from the channel was deflected by a secondary magnet through about 45° to remove neutrons and gamma rays and passed through a 1-inch polyethylene sheet to stop low-energy protons. After being thus purified the beam was defined and monitored by two 2-inch diameter scintillation counters, No. 1 and No. 2, and passed through the center of the liquid deuterium cell, as shown in Fig. 1.

The aim of this experiment was to measure only the nonradiative absorption of positive pions by deuterium, $\pi^+ + d \rightarrow p + p$, and to avoid counting any other reaction. The two protons formed in the pion absorption are emitted 180° apart in the center-of-mass system. The method of this experiment was to detect the two protons in coincidence with each other as well as in coincidence with the incident pion. Thus, the two proton counters,

²⁰ Anderson, Fermi, Martin, and Nagle, Phys. Rev. **91**, 155 (1953).

* Research supported by a joint program of the U. S. Office of Naval Research and the U. S. Atomic Energy Commission.

¹ K. A. Brueckner, Phys. Rev. **82**, 598 (1951).

² C. Morette, Phys. Rev. **76**, 1432 (1949).

³ Gunn, Power, and Tauschek, Phys. Rev. **81**, 277 (1951).

⁴ K. M. Watson and K. A. Brueckner, Phys. Rev. **83**, 1 (1951).

⁵ K. M. Watson and C. Richman, Phys. Rev. **83**, 1256 (1951).

⁶ W. B. Cheston, Phys. Rev. **83**, 1118 (1951).

⁷ Brueckner, Serber, and Watson, Phys. Rev. **84**, 258 (1951).

⁸ Chew, Goldberger, Steinberger, and Yang, Phys. Rev. **84**, 581 (1951).

⁹ A. M. L. Messiah, Phys. Rev. **86**, 430 (1952).

¹⁰ L. Van Hove and R. Marshak, Phys. Rev. **88**, 1211 (1952).

¹¹ K. M. Watson, Phys. Rev. **88**, 1163 (1952).

¹² A. H. Rosenfeld, Phys. Rev. **96**, 139 (1954).

¹³ Clark, Roberts, and Wilson, Phys. Rev. **85**, 523 (1952).

¹⁴ Durbin, Loar, and Steinberger, Phys. Rev. **84**, 581 (1951).

¹⁵ A. G. Schulz, Jr., University of California Radiation Laboratory Report UCRL-1756 (unpublished).

¹⁶ F. S. Crawford, Jr., and M. L. Stevenson, Phys. Rev. **91**, 468 (1953).

¹⁷ Cartwright, Richman, Whitehead, and Wilcox, Phys. Rev. **91**, 677 (1953).

¹⁸ Fields, Fox, Kane, Stallwood, and Sutton, Phys. Rev. **95**, 638(A) (1954).

¹⁹ A. H. Rosenfeld, Phys. Rev. **96**, 130 (1954).

No. 3 and No. 4, were placed on opposite sides of the deuterium cell and an event was recorded only when both of them fired in coincidence with the incident beam counters, No. 1 and No. 2. Counter No. 4 was large enough and was placed close enough to the cell that if one proton from a pion absorption hit counter No. 3, the other one hit No. 4 more than 99 percent of the time. The positions of the proton counters for each measurement are shown in Table I. Figure 1 is an illustration of the counters and deuterium container during the measurement of the protons at 60° in the center-of-mass system for pions of 114 Mev in the laboratory system. The double coincidences of counters No. 1 and No. 2 were recorded simultaneously with the quadruple coincidences of all four counters. The fraction of the incident beam which caused pion absorption reactions was indicated by the ratio of the quadruple to double coincidences, Q/D .

Reactions involving incident particles other than pions were prevented by purifying the beam of gamma rays, neutrons, and protons, as already described. The muons and electrons which remained in the pion beam after purification were assumed not to cause any reactions leading to quadruple coincidences. Reactions of pions with the deuterium were distinguished from those of pions with the metal walls and other surrounding materials by taking repeated measurements with the cell alternately full and empty of liquid deuterium. The difference of Q/D for these two cases was attributed to reactions of pions with the deuterium. Thus, the main problem in measuring the pion absorption was to discriminate against the other pion-deuteron reactions. The pion-deuteron reactions considered possible in this experiment were:

$$\text{nonradiative absorption} \quad \pi^+ + d \rightarrow p + p, \quad (1)$$

$$\text{elastic scattering} \quad \pi^+ + d \rightarrow \pi^+ + d, \quad (2)$$

$$\text{inelastic scattering} \quad \pi^+ + d \rightarrow \pi^+ + p + n, \quad (3)$$

$$\text{charge exchange scattering} \quad \pi^+ + d \rightarrow \pi^0 + p + p, \quad (4)$$

$$\text{radiative absorption} \quad \pi^+ + d \rightarrow \gamma + p + p. \quad (5)$$

The protons formed in reaction (1) have greater energy, hence greater range, than the protons and deuterons scattered in reactions (2), (3), and (4). A plastic absorber just thick enough to stop the most

TABLE I. Positions of proton counters and absorber thicknesses (see Fig. 1).

Laboratory energy of incident pion (Mev)	Barycentric angle between pion and proton (degrees)	Counter No.*	Laboratory angle between counter axis and incident beam (degrees)	Thickness in g/cm ² and composition of absorber in front of counter
Run No. 1				
114	45	3	37.0	5.25 Lucite
114	45	4	-125.5	2.62 Lucite
114	60	3	50.0	4.87 Lucite
114	60	4	-109.5	3.93 Lucite
114	90	3	77.8	4.12 Lucite
114	90	4	-82.5	4.87 Lucite
Run No. 2				
114	35	3	29.0	5.81 polyethylene
114	35	4	-131.7	2.07 polyethylene
114	45	3	37.0	5.81 polyethylene
114	45	4	-125.5	2.36 polyethylene
114	90	3	77.8	4.29 polyethylene
114	90	4	-82.5	4.01 polyethylene
91	35	3	29.5	4.72 polyethylene
91	35	4	-135.0	1.37 polyethylene
91	45	3	38.2	4.01 polyethylene
91	45	4	-124.2	1.65 polyethylene
91	60	3	51.5	3.73 polyethylene
91	60	4	-110.0	1.93 polyethylene
91	90	3	79.1	2.92 polyethylene
91	90	4	-80.4	2.92 polyethylene

* Counter No. 3 was always 12.5/8 inches from the center of the deuterium cell; counter No. 4 was always 6-1/2 inches from the cell.

energetic protons and deuterons from reactions (2), (3), and (4) was placed in front of each of the two proton counters, No. 3 and No. 4. The protons from reaction (1) always had enough range to penetrate the absorbers and counters, but the other reactions were almost completely prevented from counting. The thickness and composition of these absorbers for the different counters and angles measured are given in Table I and their position during a typical count is shown in Fig. 1.

The absorbers discriminated against reaction (2) very well. The scattered pion of reaction (2) has a long range and frequently triggered one of the two proton counters during the measurement. However, the recoil deuteron from the same reaction was prevented by the absorbers from reaching the other proton counter, whose simultaneous activation was required for the recording of an event.

The absorbers did not discriminate completely against reactions (3), (4), and (5) and a few quadruple coincidences are caused by them. The rest of this section is a discussion of the corrections required to compensate for these spurious counts (which constituted about 3 percent of the quadruples).

The recoil proton of reaction (3) was always stopped by the absorbers, but both the scattered pion and the recoil neutron could penetrate the absorbers. The pion frequently fired one of the proton counters and it was possible for the neutron, by causing a star in the counter or by knocking a proton from either the counter or its

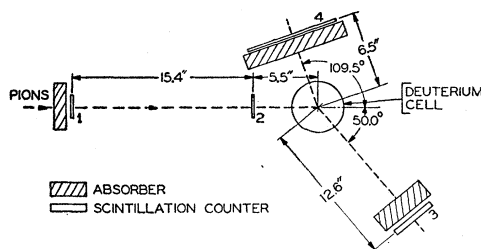


Fig. 1. Experimental arrangement for angular distribution measurement.

absorber into the counter, to fire the second proton counter simultaneously. Whenever this chain of events occurred it was recorded as a quadruple coincidence. The frequency of this type of event has been calculated from the measured cross section for negative pion scattering by deuterium at this energy²¹ to be about 2.7 percent of the net Q/D rate.

The protons formed in reaction (4) are both prevented from reaching the counters. However, there is a small chance that the two gamma rays formed by the decay of the neutral pion²¹ will each create a pair directed at one of the two proton counters. The contribution of this occurrence to the net counting rate was calculated to be 0.2 percent.

The radiative absorption, reaction (5), is a very slow reaction at the energy of this experiment. If it is assumed that the radiative absorption of positive pions by deuterons is the same as that by neutrons, then reaction (5) is the inverse reaction of the photoproduction of positive pions from protons. On this assumption, the cross section of reaction (5) was estimated by detailed balancing from the measured cross section for the photoeffect²² to be 1.8×10^{-2} mb/sterad. Reaction (5) usually forms a high-energy gamma ray and protons too slow to be counted. Occasionally it forms a low-energy gamma ray and two oppositely directed, high-energy protons which penetrate both proton counters and cause an event to be recorded. The contribution of reaction (5) to the total counting rate was estimated to be 0.1 percent. On the basis of the above considerations it was concluded that reaction (1) was counted with very good efficiency (calculated in Sec. VI) and that all other reactions contributed only a very small number of counts.

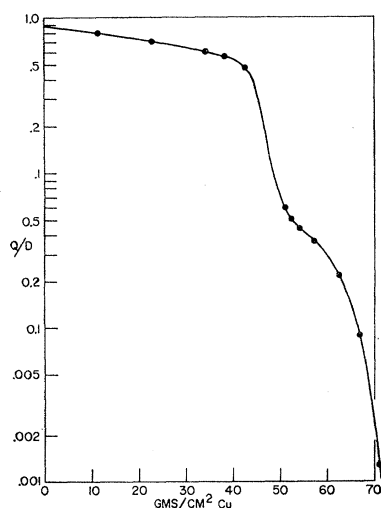


FIG. 2. Range curve of π^+ in copper.

²¹ D. E. Nagle, Phys. Rev. **93**, 918 (1954).

²² Bishop, Steinberger, and Cook, Phys. Rev. **80**, 291 (1950).

III. ENERGY OF THE PION BEAM

The energy of the pion beam is determined by the position of the beryllium target inside the cyclotron, by the strength of the cyclotron magnetic field, and by the position of the channel cut in the shield wall through which the pions are permitted to emerge into the experimental area.²³ These parameters were set before the experiment to give approximately the desired energy of positive pions in the channel. The exact energy of the pions was measured by range curves taken immediately before each set of angular distribution measurements. Figure 2 shows a representative range curve. For this measurement counters No. 1 and No. 2 and the polyethylene absorber between the secondary magnet and counter No. 1 were left in their standard positions (see Fig. 1). The deuterium cell was removed and counters No. 3 and No. 4 were placed in line with and behind counters No. 1 and No. 2. (counter No. 4, the larger one, was placed last to reduce losses caused by multiple scattering.) Copper absorbers 10 inches high by 10 inches wide and of various thicknesses were inserted between counter No. 2 and counter No. 3. Attenuation measurements were made by recording double coincidences of counters No. 1 and No. 2, and quadruple coincidences of all four counters. Figure 2 is a plot of the ratio of quadruple to double coincidences *versus* thickness of copper absorber used. The curve shows a sharp drop corresponding to the end of the pion range with a secondary plateau and another sharp drop corresponding to the end of the range of the remaining muons. The uncorrected mean range of the pions from the curve is 46.2 g/cm² of copper. The residual range of the pions at the center of the deuterium cell during the angular distribution measurement is obtained by adding to the copper the thickness of counter No. 3 plus one-half the thickness of counter No. 4 minus one-half the thickness of the deuterium cell, including walls. This corrected range is then converted to energy, by means of the range energy tables of Aron²⁴ and by adopting 6.72²⁵ as the mass ratio of the proton to the pion, which gives an energy of 114 ± 5 Mev in the laboratory system.

The range curves were also used to estimate the contamination of the beam by muons and electrons. The total contamination was estimated to be 4.3 ± 2.0 percent at 114 Mev and 5.0 ± 2.0 percent at 91 Mev, so the pion fractions were taken to be 0.957 ± 0.02 and 0.950 ± 0.02 , respectively.

IV. LIQUID DEUTERIUM CONTAINER

Figure 3 is a schematic cross section of the liquid deuterium container. The container is a metal Dewar with a good vacuum between the outer wall and the

²³ R. L. Martin, Phys. Rev. **87**, 1052 (1952).

²⁴ W. A. Aron, University of California Radiation Laboratory Report UCRL-1325 (unpublished).

²⁵ Smith, Birnbaum, and Barkas, Phys. Rev. **91**, 765 (1953).

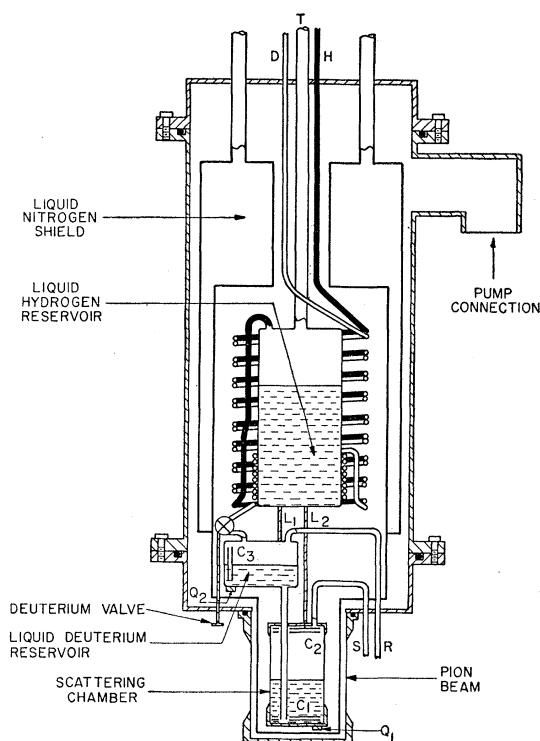


FIG. 3. Liquid deuterium container.

inner containers of hydrogen and deuterium. A metal radiation shield, kept at liquid nitrogen temperature, is suspended between the outside wall and the inner containers to reduce heat radiation to the deuterium and hydrogen. Deuterium gas is cooled and liquefied in a heat exchanger which surrounds the liquid hydrogen reservoir. The liquid deuterium trickles down through the deuterium valve into the liquid deuterium reservoir and scattering chamber where it remains throughout the experiment. The walls surrounding the scattering cell were made thin to reduce background scattering. The outside wall was 0.030-inch aluminum and the radiation shield was 0.002-inch aluminum. The cell wall was 0.005-inch brass, in its thin-walled part, which was $4\frac{1}{4}$ inches in diameter and $4\frac{1}{4}$ inches high. The cell had a capacity of 1.14 liters; the reservoir, which had a slightly greater capacity than the cell, was connected to it by a tube extending from the bottom of the reservoir nearly to the bottom of the cell. There was a vapor exhaust tube leading out from the top of the cell and a similar one leading out from the top of the reservoir. Whenever it was required to empty the cell, the cell vapor exhaust line was closed, the reservoir vapor exhaust line was opened, and a 15-watt electric heater, Q_1 , at the bottom of the cell was turned on. The vapor evolved in the cell forced the liquid deuterium up into the reservoir in about two minutes. The heater power was then reduced to the two watts required to hold the deuterium up in the reservoir. When it was

desired to refill the cell, the cell exhaust line was opened, the reservoir line closed, the cell heater turned off, and a 15-watt heater, Q_2 , at the bottom of the reservoir was turned on. The liquid then returned to the cell under the vapor pressure in the reservoir and gravity in a similar time. By this method successive counts were taken with the cell alternately full and empty of deuterium liquid.

The indication that the cell was full of liquid deuterium was the increase in capacity of four micromicrofarads in a horizontal parallel plate condenser, C_2 , at the top of the cell, above the thin-walled section. The indication that the cell was empty was the decrease in capacity of the same amount in a similar condenser, C_1 , at the bottom of the cell.

The path length of the pions through the cylindrical deuterium cell was averaged over the beam using a beam profile measured at the position of the scattering cell, and the mean path length was found to be 10.2 cm. The liquid deuterium contained $(4.84 \pm 0.04) 10^{22}$ atoms per cm^3 . When the cell was empty of liquid it contained deuterium vapor amounting to $(0.08 \pm 0.01) 10^{22}$ atoms per cm^3 . The difference, $(4.76 \pm 0.05) 10^{22}$, multiplied by the mean path length, gives $(4.87 \pm 0.05) 10^{23}$ deuterium atoms per cm^2 . The uncertainty in the densities of the liquid and vapor is the result of uncertainty about their temperature.

V. COUNTING EQUIPMENT

Liquid and plastic scintillation counters were used in this experiment because they can be made nearly 100 percent efficient for meson and proton counting over a large sensitive area and because they are quite fast. The scintillating liquid used in counters No. 1 and No. 3 was phenylcyclohexane with 3 grams per liter of *p*-terphenyl and 10 milligrams per liter of diphenylhexatriene.²⁶ The cell of No. 1 was 1/4-inch thick overall with 1/32-inch Lucite windows cemented into a Lucite frame, holding a cylindrical volume of scintillating liquid 2 inches in diameter by 3/16 inch thick. The cell of No. 3 was 1/2-inch thick overall, with 1/16-inch windows, holding a cylindrical volume of liquid 4 inches in diameter and 3/8 inch thick. One end of each Lucite cell was shaped to fit the photocathode of an RCA 5819 photomultiplier tube. The cell was pressed against the tube and a thin layer of silicone grease between them assured good optical contact.

Counters No. 2 and No. 4 used plastic scintillators, cut from scintillating plastic sheet. Counter No. 2 had a sensitive volume 2 inches in diameter and 1/8 inch thick, clamped tightly inside one end of a Lucite light pipe shaped to fit the lateral surface of the plastic cylinder. The other end of the light pipe made good optical contact with the RCA 5819 photocathode. Counter No. 4 had a 6 inches high by 8 inches wide by 1/8 inch thick plastic scintillator clamped to one end of

²⁶ H. Kallman and M. Furst, Phys. Rev. **81**, 853 (1951).

TABLE II. Observed values of Q/D , the fraction of pions non-radiatively absorbed, in units of 10^{-6} .

Run No.	Pion energy in laboratory frame (Mev)	Barycentric angle between pion and proton (degrees)	With deuterium	Without deuterium	Net
1	114	45	85.4±6.5	12.0±4.0	73.4±8.3
1	114	60	61.5±3.9	8.0±3.0	53.5±4.9
1	114	90	32.0±4.0	2.3±1.5	29.7±4.3
2	114	35	124.0±6.0	12.0±4.0	112.0±7.1
2	114	45	104.3±5.6	15.2±4.0	89.1±6.9
2	114	90	37.5±4.3	5.4±3.8	32.1±5.7
2	91	35	111.9±7.0	17.5±6.0	94.4±9.2
2	91	45	75.3±6.0	10.9±4.0	64.4±7.1
2	91	60	50.3±5.0	13.4±3.3	36.9±6.0
2	91	90	24.2±3.5	1.9±1.9	22.3±4.0

a Lucite light pipe whose other end made good optical contact with an RCA 5819 photocathode. The scintillators and light pipes of all the counters were covered with thin aluminum foil sealed with black electrical Scotch Tape to keep stray light out and to increase the collection of scintillated light. The photomultiplier tube of each counter was surrounded by a cylindrical iron shield to protect it from the stray magnetic field of the cyclotron.

The photomultiplier anode of each counter was connected to a preamplifier which clipped the pulses into a fairly square shape 2×10^{-8} second wide. These pulses were amplified by four stages of distributed amplification²⁷ before being delivered to the coincidence circuits.²⁷ The pulses from counters No. 1 and No. 2 were fed into a coincidence circuit *A*; the pulses from No. 2 and No. 3 were fed into a circuit *B*; and the pulses from No. 1 and No. 4 were fed into a coincidence circuit *C*. The output pulses from circuits *A*, *B*, and *C* were counted in triple coincidence and recorded by a cascade combination of a Hewlett Packard high-speed scaler and an Atomic Instrument decade scaler as Q , the quadruple coincidences of all four counters. The output pulses of coincidence circuit *A* were simultaneously counted by a similar cascade of scalers and recorded as D , the double coincidences of counters No. 1 and No. 2. Coincidence circuits *A*, *B*, and *C* were double coincidence circuits with triggered output pulses about 5×10^{-8} second long.²⁷ The counting rates were low enough (10^4 per second during cyclotron pulses) and the dead time of the counting equipment short enough (10^{-7} second) that counting losses were negligible.

There was enough stray radiation in the experimental room to cause some accidental coincidences even though the resolving time of the coincidence equipment for quadruple coincidences was 6×10^{-8} second. These were computed from the measured singles, doubles, and triples rates of all counters and the measured resolving

time of the coincidence circuits involved and were found to range from 0.8 to 1.3 quadruple coincidences per million incident particles at a beam rate of 10^4 per minute. The contribution of accidental coincidences, calculated from the actual incident-beam rate during the angular-distribution measurements, was subtracted from the values of Q/D on Table II before recording them on Table III. The correction ranged from 0.8 to 2.0 percent at 114 Mev and from 2.3 to 7.6 percent at 91 Mev.

It was necessary to know the efficiency of the counting equipment for protons traversing any part of the sensitive area of counters No. 3 and No. 4. To estimate this the current at the photomultiplier anode of each counter was measured while a 1/4-inch diameter beam of Co^{60} gamma rays was passed through the scintillator at various points both near and far from the photocathode. The response of counter No. 3 measured in this way was nearly uniform all over its area. The current produced by counter No. 4 was twice as great for particles traversing the photocathode end of the scintillator as it was for those traversing the opposite end. The amplifications of the photomultipliers were adjusted to make the pulses delivered to the coincidence circuits twice the threshold size required by those circuits when 110-Mev mesons passed through the center of the counters. The efficiency of counters No. 3 and No. 4 for these mesons was measured directly, by placing them in line with and between counters No. 1 and No. 2 in the meson beam. The ratio of quadruple coincidences of all counters to double coincidences of counters No. 1 and No. 2 was (0.975 ± 0.002) . The protons counted during the angular distribution measurement gave up four times as much energy to the counters as did these mesons, so it was assumed that they were counted with 100 percent efficiency all over the counter area.

TABLE III. Differential cross sections for pion absorption.

$$\frac{d\sigma}{\omega d} = \frac{Q}{D} \frac{1-r}{2n\Omega efb},$$

where $n = 4.87 \times 10^{23}$ deuterium atoms/cm², $\Omega = 0.0776$ steradian, $f = 0.957$ at 114 Mev and 0.950 at 91 Mev = pion content of the beam, $b = 0.994$ = correction for absorption of the beam by deuterium, and $r = 0.030$ = fraction of quadruple coincidences due to pion scattering reactions.

<i>E</i> Mev	θ degrees	$10^6 \times \text{Net } Q/D^a$ Fraction of pions absorbed	e detection efficiency	Differential cross section $\frac{d\sigma}{\omega d}$, (10^{-27} cm ² per steradian)	
				Laboratory system	Barycentric system
114	35	111.0±7.1	0.895	1.680±0.107	1.189±0.076
114	45	82.6±5.3	0.883	1.267±0.080	0.926±0.058
114	60	52.6±5.0	0.866	0.823±0.078	0.643±0.061
114	90	29.8±3.5	0.860	0.470±0.055	0.442±0.052
91	35	91.7±9.3	0.907	1.380±0.140	1.010±0.102
91	45	62.9±7.1	0.905	0.949±0.107	0.718±0.081
91	60	35.2±6.0	0.897	0.536±0.091	0.431±0.073
91	90	20.6±4.0	0.894	0.315±0.061	0.300±0.058

^a Corrected for accidental coincidences.²⁷ Glicksman, Anderson, and Martin, Proc. Natl. Electronics Conf. 9, 483 (1954).

VI. DIFFERENTIAL CROSS SECTIONS

The measurement of pion absorption was carried out for two energies of the primary beam, 91 and 114 Mev in the laboratory system. At each of these energies measurements of Q/D , the ratio of quadruple to double coincidences, were made at center-of-mass angles of 35° , 45° , 60° , and 90° between the forward proton and the incident beam. At each position measurements were made both with and without deuterium in the scattering cell and the difference of the two results attributed to protons from the pion absorption by the deuterium. It was pointed out in Sec. II that only 3 percent of the counts were caused by other processes. The observed values of Q/D are listed in Table II.

The differential cross section in the laboratory system is found from Q/D by the following formula:

$$\frac{d\sigma}{d\omega} = \frac{Q}{D} \frac{1-r}{2nfb\Omega e}.$$

In this formula n is the number of deuterium atoms per cm^2 , 4.87×10^{23} , as computed in Sec. IV; f is the fraction of the incident beam which is pions, 0.957 ± 0.020 at 114 Mev and 0.950 ± 0.020 at 91 Mev (see Sec. III); and the factor $b = 0.994$ is a correction for the absorption of the beam by the deuterium. r is the fraction of quadruples counts caused by various scattering reactions (calculated to be 3.0 percent in Sec. II). Ω is the effective solid angle accepted by counters No. 3 and No. 4 and e is their combined efficiency. Counter No. 3 is 4 inches in diameter and was placed 12 5/8 inches from the center of the scattering cell; counter No. 4 is 6 inches high by 8 inches wide and was placed 6 1/2 inches from the cell. Thus, counter No. 3 nearly defined the solid angle accepted by both counters, which was 0.0776 steradian.

The efficiency of counters No. 3 and No. 4 for counting a pair of protons that geometrically should have been accepted by both counters was not 100

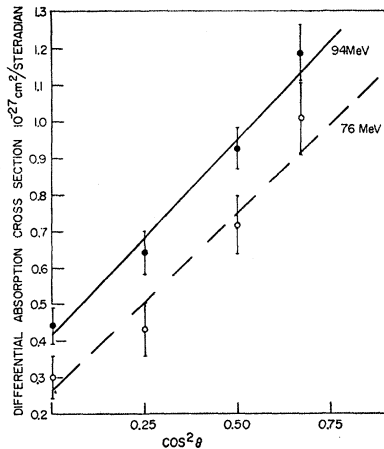


FIG. 4. Differential cross sections at 94 and 76 Mev in the barycentric system plotted versus $\cos^2 \theta$.

TABLE IV. Angular distributions and total cross sections.

$$\frac{d\sigma}{d\omega} = \alpha_1 + \alpha_2 \cos^2 \theta.$$

E Pion energy in Bary- centric system Mev	α_1 $10^{-27} \text{ cm}^2/\text{sterad}$	α_2 $10^{-27} \text{ cm}^2/\text{sterad}$	$a = \frac{\alpha_1}{\alpha_2}$	M Least squares sum	σ Integrated total cross section 10^{-27} cm^2
76	0.262 ± 0.053	0.978 ± 0.150	0.268 ± 0.089	2.40	7.38 ± 1.20
94	0.415 ± 0.047	1.071 ± 0.120	0.388 ± 0.082	1.45	9.70 ± 1.03

percent, even though every proton had sufficient range to penetrate the counters, because of nuclear absorption in the deuterium cell and the absorbers. In order to compute this loss, the cross sections of these materials for the absorption of protons were assumed to be the same as their absorption cross sections for neutrons, i.e., one half their total cross sections for neutrons, except for hydrogen whose proton absorption was assumed to be nil. The neutron cross sections were found by interpolation between the values of Cook *et al.*,²⁸ De Juren and Knable,²⁹ and Taylor *et al.*³⁰ The loss of quadruple coincidences caused by absorption was found to be from 10.0 percent to 14.1 percent, depending on the proton energy and absorber thickness. Diffraction scattering by the deuterium also reduced the efficiency a small amount (0.7 to 0.9 percent at the various angles). Both the total efficiency, e , and the differential cross sections, for the various angles and incident pion energies, are given in Table III.

VII. ANGULAR DISTRIBUTIONS AND TOTAL CROSS SECTIONS

In Fig. 4, the differential cross sections in the barycentric system are plotted against $\cos^2 \theta$, where θ is the barycentric angle between the pion and proton directions. At the energies of this experiment there may be small interactions in the d state as well as those in the s and p states found at lower energies. Thus, the differential cross sections can be represented by

$$\frac{d\sigma}{d\omega} = \alpha_1 + \alpha_2 \cos^2 \theta + \alpha_3 \cos^4 \theta.$$

If α_3 is assumed zero, a least-squares analysis of the data gives values of M , the least-squares sum, of the order of the difference between the number of points and the number of parameters, indicating a good fit. However, this does not rule out even a fairly substantial α_3 , since a wide range of positive values of α_3 give better fits than $\alpha_3 = 0$. The actual value of α_3 is not determined well by this experiment because the statistical errors are fairly large and because the $\cos^4 \theta$ term would not contribute very much at the large angles

²⁸ Cook, McMillan, Peterson, and Sewell, Phys. Rev. **75**, 7 (1949).

²⁹ J. De Juren and N. Knable, Phys. Rev. **77**, 606 (1950).

³⁰ Taylor, Pickavance, Cassels, and Randle, Phil. Mag. **42**, 20 (1951).

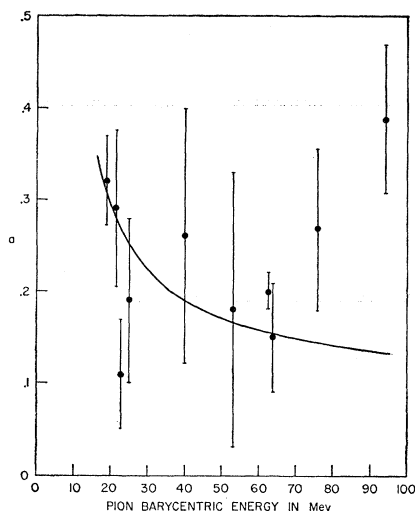


FIG. 5. The coefficient a plotted versus pion energy. The curve is proportional to η^{-2} where η is the pion momentum divided by μc . It is fitted to the experimental values below 70 Mev. (See reference 12.)

(35° and larger) which could be measured without interference from the incident beam. The value of α_2 given by the least-squares analysis depends very strongly on the assumed value of α_3 , because the observed anisotropy of the angular distribution can be assumed dependent on either $\cos^2\theta$ or $\cos^4\theta$. On the assumption that α_3 is zero, one obtains values of $a = \alpha_1/\alpha_2$ of 0.268 ± 0.089 and 0.388 ± 0.082 at pion energies of 76 and 94 Mev in the center-of-mass system. Table IV shows the values found for α_1 , α_2 , a , and the least-squares sum, M , on the assumption that α_3 is zero.

The differential cross sections were integrated over solid angle to give the total cross sections shown in Table IV. As an over-all check the integrated total cross section found in this experiment at 114 Mev in the laboratory system was added to the sum of the integrated cross sections for ordinary and charge exchange scattering of negative pions at 120 Mev²¹ and compared to the total cross section of deuterium for pions found by transmission measurements. The two values agree within experimental errors.

In Fig. 5 the parameter $a = \alpha_1/\alpha_2$, where $d\sigma/d\omega = \alpha_1 + \alpha_2 \cos^2\theta$, is plotted against pion energy in the center-of-mass system. The values shown have been taken from both the direct reaction,^{13,14} $\pi^+ + d \rightarrow p + p$, and its inverse.¹⁵⁻¹⁹ It has been suggested^{11,12} that at low energies the parameter a should decrease with increasing energy as η^{-2} . However, the value of a found at 94 Mev

in the present experiment is considerably larger than is predicted by an η^{-2} dependence. The smooth variation of a with energy from 65 Mev to 94 Mev through values measured under identical experimental conditions indicates that the increase of a with energy is real. This in turn indicates that the region in which a is proportional to η^{-2} is limited to pion energies of less than 90 Mev in the barycentric system.

In Fig. 6 the integrated total cross section, σ , is plotted against barycentric energy of the pion. The values have been taken from measurements of both the absorption reaction^{13,14} and, by detailed balancing, from those of its inverse, the pion production reaction.¹⁵⁻¹⁹ The two highest-energy points, the results of the present experiment, lie on a smooth extrapolation of the excitation function found by earlier workers.

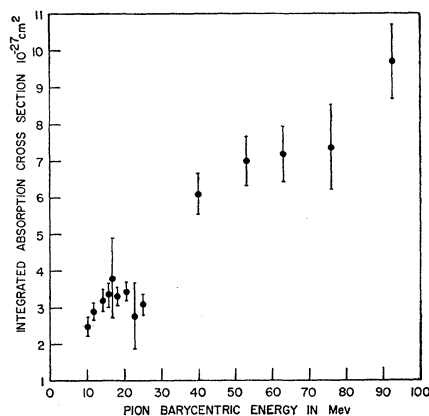


FIG. 6. Integrated total cross sections plotted versus pion energy.

The present measurements of the reaction $\pi^+ + d \rightarrow p + p$ at 76 and 94 Mev in the barycentric system show:

(a) The angular distribution of the protons can be represented by $a + \cos^2\theta$. The angular distribution becomes more isotropic with increasing energy above 70 Mev, reversing the trend at lower energies.

(b) The total cross section continues to increase with energy up to 94 Mev.

It is a pleasure to acknowledge the help and guidance of Dr. D. E. Nagle, who suggested this problem. Thanks are also due Dr. Earl Long and Dr. Lothar Meyer for liquid hydrogen, Dr. H. L. Anderson for the use of his counting equipment, and Mr. W. Skolink, Mr. C. Cohn, Dr. M. Glicksman, and Mr. G. B. Yodh for helping to carry out the measurements.